

# Orbital ordering transition in $\text{Ca}_2\text{RuO}_4$ observed with resonant x-ray diffraction

I. Zegkinoglou<sup>1</sup>, J. Stremper<sup>1</sup>, C.S. Nelson<sup>2</sup>, J.P. Hill<sup>3</sup>, J. Chakhalian<sup>1</sup>, C. Bernhard<sup>1</sup>,  
J.C. Lang<sup>4</sup>, G. Srajer<sup>4</sup>, H. Fukazawa<sup>5</sup>, S. Nakatsuji<sup>5</sup>, Y. Maeno<sup>5,6</sup>, and B. Keimer<sup>1</sup>

<sup>1</sup> *Max-Planck-Institut für Festkörperforschung, Heisenbergstr. 1, D-70569 Stuttgart, Germany*

<sup>2</sup> *National Synchrotron Light Source, Brookhaven National Laboratory, Upton, New York 11973-5000, USA*

<sup>3</sup> *Department of Physics, Brookhaven National Laboratory, Upton, New York 11973-5000, USA*

<sup>4</sup> *Advanced Photon Source, Argonne National Laboratory, Argonne, Illinois 60439, USA*

<sup>5</sup> *Department of Physics, Kyoto University, Kyoto 606-8502, Japan and*

<sup>6</sup> *International Innovation Center, Kyoto University, Kyoto 606-8501, Japan*

(Dated: November 21, 2018)

Resonant x-ray diffraction performed at the  $L_{II}$  and  $L_{III}$  absorption edges of Ru has been used to investigate the magnetic and orbital ordering in  $\text{Ca}_2\text{RuO}_4$  single crystals. A large resonant enhancement due to electric dipole  $2p \rightarrow 4d$  transitions is observed at the wave-vector characteristic of antiferromagnetic ordering. Besides the previously known antiferromagnetic phase transition at  $T_N = 110$  K, an additional phase transition, between two paramagnetic phases, is observed around 260 K. Based on the polarization and azimuthal angle dependence of the diffraction signal, this transition can be attributed to orbital ordering of the Ru  $t_{2g}$  electrons. The propagation vector of the orbital order is inconsistent with some theoretical predictions for the orbital state of  $\text{Ca}_2\text{RuO}_4$ .

PACS numbers: 75.25.+z, 71.27.+a, 75.30.-m, 61.10.-i

The discovery of high temperature superconductivity in layered cuprates has stimulated a great deal of interest in the electronic properties of transition metal oxides (TMOs) in recent years. Among these, 4d electron systems such as the two-dimensional Mott transition system  $\text{Ca}_{2-x}\text{Sr}_x\text{RuO}_4$  are particularly interesting. The strong correlations induced by the narrow electron bands, the active orbital degree of freedom, and the unconventional superconductivity discovered in the  $x = 2$  end member of this system [1, 2] are some of the properties which have motivated its extensive study. Magnetic and orbital ordering are expected to be intimately coupled in 4d compounds, and resonant x-ray diffraction (RXD) is well suited to elucidate the interplay between these two degrees of freedom. RXD experiments performed at energies close to the K-absorption edges of transition metals have been used to study orbital and magnetic ordering in 3d TMOs [3, 4, 5, 6]. A much larger resonant enhancement of the diffracted intensity is expected at the L-edges of transition metals, because the partially filled d-electron orbitals are then directly probed by electric dipole transitions. This can enable the direct observation of orbital ordering. Such experiments have recently been performed on compounds with 3d [7, 8, 9] and 5d [10] valence electrons, but no measurements on 4d electron materials have been reported to date.

Here we report the results of a RXD study at the L-edges of Ru, a 4d transition metal, in the Mott insulator  $\text{Ca}_2\text{RuO}_4$  [11]. Several controversial predictions have been made for the ordering of the 4d  $t_{2g}$  Ru orbitals in this system [12, 13, 14, 15, 16], which provide a strong motivation for this investigation. We observed a pronounced resonant enhancement at the Ru  $L_{II}$  (2.9685 keV) and  $L_{III}$  (2.837 keV) edges of the magnetic scattering intensity at the wave-vector where antiferromagnetic

(AF) order had been reported by neutron powder diffraction [17]. Significant resonant intensity was observed also above the Néel temperature,  $T_N = 110$  K, vanishing at a second phase transition at a much higher temperature,  $T_{OO} = 260$  K. We attribute this transition, which has not previously been observed, to orbital ordering. The orbital order is characterized by the same propagation vector as the low-temperature AF state. At wave-vectors corresponding to theoretically predicted orbital ordering patterns with larger unit cells [13], no signal was observed.

The crystal structure of  $\text{Ca}_2\text{RuO}_4$  is based on  $\text{RuO}_2$  layers built up of corner-sharing  $\text{RuO}_6$  octahedra. At  $T_M = 357$  K, the material undergoes a first-order transition from a high-temperature metallic to a low-temperature insulating phase [11, 18, 19]. This transition is accompanied by a structural transition from tetragonal to orthorhombic lattice symmetry, which leads to a contraction of the  $\text{RuO}_6$  octahedra perpendicular to the  $\text{RuO}_2$  layers [19]. The Ru spins order antiferromagnetically below  $T_N = 110$  K [11, 17, 20]. In the following, the wave-vector components ( $hkl$ ) are indexed in the orthorhombic space-group  $Pbca$ . The room temperature lattice constants are:  $a = 5.4097(3)$  Å,  $b = 5.4924(4)$  Å, and  $c = 11.9613(6)$  Å [17]. In this notation, the AF order is characterized by the propagation vector (100).

The experiments were conducted at beamline 4ID-D of the Advanced Photon Source at Argonne National Laboratory. The storage ring chamber at this station was modified to allow measurements at energies as low as 2.6 keV, and the beam path was optimized to minimize the absorption of the x-ray beam by air. The sample was mounted in a closed-cycle cryostat capable of reaching temperatures between 10 and 350 K, on an 8-circle diffractometer. A Si (111) crystal was used as polariza-

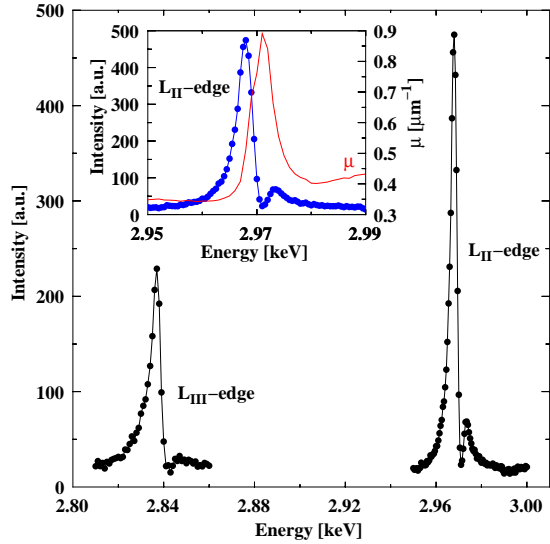


FIG. 1: Energy dependence of the scattered intensity of the (100)-reflection around the  $L_{II}$  and  $L_{III}$  absorption edges at a sample temperature of 20 K ( $\psi = 0^\circ$ ). The energy profiles are not corrected for absorption. The inset shows the  $L_{II}$  resonance in more detail, together with the absorption coefficient  $\mu$  (right scale), calculated from fluorescence measurements.

tion analyzer, providing scattering angles of  $\theta = 41.8^\circ$  and  $\theta = 44.2^\circ$  at the  $L_{II}$  and  $L_{III}$  absorption edges, respectively. This results in a suppression of the complementary polarization component of the beam by 2 and 3 orders of magnitude, respectively, for the  $L_{II}$  and  $L_{III}$  edges, which is sufficient for the separation of the two components. Two single-crystal samples grown with the floating-zone method [21] were used for the experiments, with sizes of approximately  $100 \times 100 \times 50 \mu\text{m}^3$  and  $500 \times 400 \times 50 \mu\text{m}^3$ . The probing depth of  $\text{Ca}_2\text{RuO}_4$  in this energy range is of the order of  $2 \mu\text{m}$ . The alignment of the samples was carried out with the  $\lambda/3$  harmonic component of the incident beam using the (200) or (220) main Bragg reflections.

The energy dependence of the diffracted intensity at the magnetic ordering wave-vector (100) is shown in Fig. 1. The measurements were taken at 20 K, without a polarization analyzer and with the magnetic moment of the sample ( $\vec{\mu} \parallel \vec{b}$ ) in the scattering plane. In the following, we define this azimuthal position as  $\psi = 0^\circ$ . The data shown are not corrected for absorption. Strong resonances are observed at both the Ru  $L_{II}$  and  $L_{III}$  absorption edges. No off-resonance scattering was observed at the (100) position within the experimental sensitivity. The resonance enhancement at the Ru  $L_{II}$  edge is thus at least a factor of 500. This enhancement originates from electric dipole  $2p \rightarrow 4d$  transitions that probe directly the partially filled 4d orbitals responsible for magnetism. When the sample is rotated around the scattering vector to  $\psi = 90^\circ$ , the magnetic signal vanishes completely. The azimuthal dependence of the scattered intensity (not

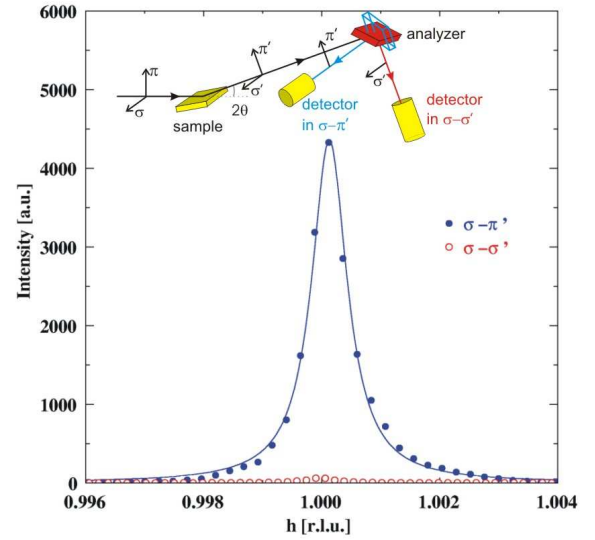


FIG. 2: Polarization dependence of the scattered intensity at the (100) position at  $\psi = 0^\circ$ . Data are shown for the  $\sigma - \pi'$  (full bullets) and  $\sigma - \sigma'$  (empty bullets) polarization channels. The solid line is the result of a fit to a Lorentzian profile. The inset shows a schematic view of the experimental configuration.

shown) is consistent with the one expected for dipole resonant magnetic scattering [22, 23].

The inset in Fig. 1 shows the energy scan around the  $L_{II}$  edge in more detail. In addition to the resonance peak at the absorption edge ( $L_{II} = 2.9685 \text{ keV}$ ), the data reveal a second peak, 4 eV higher in energy ( $L_{II}' = 2.9725 \text{ keV}$ ). The origin of this peak will be addressed below. For comparison, the solid line in the graph shows the energy dependence of the absorption coefficient  $\mu$  around the  $L_{II}$  edge, as calculated from fluorescence measurements following Ref. 27. The inflection points of the fluorescence curve coincide with the two peaks of the energy scan.

Reciprocal-space scans along the  $h$ -direction conducted at the (100) position at  $L_{II}$  and  $\psi = 0^\circ$  at low temperatures are shown in Fig. 2, both for the  $\sigma - \pi'$  and for the  $\sigma - \sigma'$  polarization geometry. Here  $\sigma$  and  $\pi$  denote the polarization components perpendicular and parallel to the diffraction plane, respectively (inset Fig. 2). Significant intensity is observed only in  $\sigma - \pi'$ . The weak intensity found in  $\sigma - \sigma'$  is due to leakage from the  $\sigma - \pi'$  channel ( $\sim 1\%$ ), due to the fact that the scattering angle of the analyzer at this energy is not exactly  $45^\circ$ . The absence of any  $\sigma - \sigma'$  intensity at  $\psi = 0^\circ$  and the absence of the reflection at  $\psi = 90^\circ$  indicate that there is no charge scattering contribution to the (100) intensity.

Fig. 3 shows the temperature dependence of the integrated intensity obtained from  $h$ -scans conducted at the (100) position at  $L_{II}$  both with the analyzer in  $\sigma - \pi'$  geometry and without an analyzer (Fig. 3a), as well as at  $L_{II}'$  without an analyzer (Fig. 3b). At  $L_{II}$  the previously known magnetic transition at  $T_N = 110 \text{ K}$  is clearly

observed. Remarkably, however, the intensity does not drop to zero above  $T_N$ . Right above  $T_N$ , it is about a factor of 20 lower than the intensity at 10 K. It then decreases smoothly with increasing temperature and vanishes around 260 K in an order-parameter-like fashion (Fig. 3a; note the logarithmic scale). This indicates a second phase transition that has thus far not been reported. As discussed below, we attribute the intensity above 110 K to orbital ordering of the Ru  $t_{2g}$  electrons. As is the case below  $T_N$ , the intensity for  $T_N < T < 260$  K is observed only in the  $\sigma - \pi'$  channel and vanishes when the sample is rotated to  $\psi = 90^\circ$ . This means that there is no significant charge scattering at the (100) position in this new phase.

Energy scans conducted at temperatures below  $T_N$ , just above  $T_N$ , and at  $T = 290$  K are shown in Fig. 3c. All scans were corrected for absorption by multiplying the raw data by the square of the energy-dependent absorption coefficient, as discussed in Refs. 25, 26. The line shape above  $T_N$  is quite different from that below, strongly suggesting that this new scattering is not magnetic in origin.

In order to test this, muon spin rotation ( $\mu$ SR) experiments were performed on single crystals of the same origin as the ones used in the diffraction experiments. The measurements were carried out at the GPS beamline at the Paul Scherrer Institute (PSI), Switzerland. No measurable static magnetic moment was found above the Néel temperature. The detection limit of this technique is one order of magnitude lower than the magnitude of the magnetic moment that would be expected for the second phase if it were magnetic, based on the intensity ratio below and above  $T_N$ . The phase between  $T = T_N$  and  $T_{OO} = 260$  K is thus paramagnetic. Based on this conclusion and on the absence of charge scattering at (100), we attribute the 260 K transition to the ordering of the Ru 4d  $t_{2g}$  orbitals. We note that such an ordering, which would modify the spin Hamiltonian and hence the paramagnetic fluctuations, may also explain anomalies in the uniform susceptibility of  $\text{Ca}_2\text{RuO}_4$  previously reported around 260 K [21].

The data presented thus far indicate the presence of orbital order below  $T_{OO} = 260$  K characterized by the same propagation vector as the AF order that sets in below 110 K. Motivated by the theoretical prediction of an orbitally ordered state with a larger unit cell [13], we also carried out searches for resonant diffraction at reciprocal space positions consistent with the suggested ordering pattern. However, no reflections were observed either at  $(1/2 \ 1/2 \ 0)$  or at  $(1/2 \ 1/2 \ 1/2)$ . This scenario therefore does not appear to be viable for  $\text{Ca}_2\text{RuO}_4$ . While orbital order with the observed (100) propagation vector has not been theoretically predicted, a “ferro-orbital” component of the ordering pattern [15, 16, 24] cannot be ruled out.

Besides the new phase observed at (100) below 260 K, a resonance peak was also found at the (110) posi-

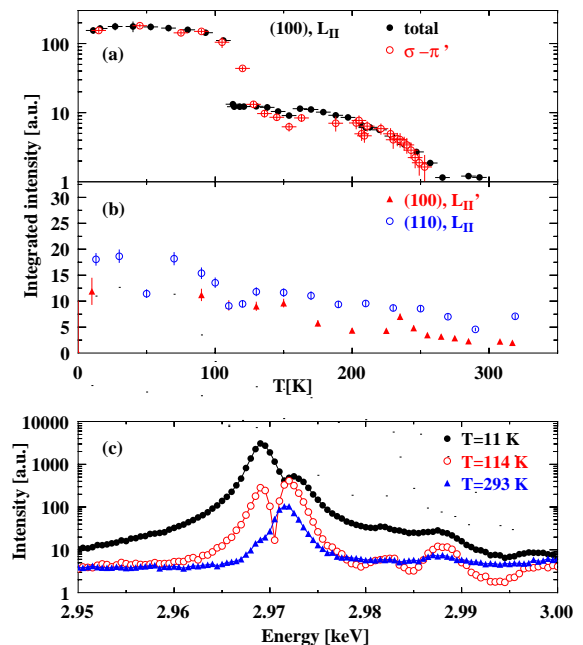


FIG. 3: Temperature dependence of the integrated intensity of the (100) peak as determined from  $h$ -scans, at (a)  $L_{II}$ , both without analyzer and in  $\sigma - \pi'$  geometry (scaled), as well as (b) at  $L_{II}'$ . In (a), the measurements with and without polarization analyzer were taken on two different samples. The horizontal error bars reflect uncertainties about the thermal coupling between sample, cold finger and temperature sensors. In (b), because of the strong contribution from the  $L_{II}$  resonance peak, the integrated intensity at  $L_{II}'$  could be reliably determined from  $h$ -scans only above 90 K. The intensity at  $T = 10$  K has therefore been determined from energy scans (panel c). In (b) the temperature dependence of the (110) peak at  $L_{II}$  is also shown. (c) Variation of the intensity of the (100) peak with energy around the  $L_{II}$ -edge for selected temperatures. All scans were corrected for absorption.

tion, which is not allowed by the  $Pbca$  space-group and is also magnetically forbidden. The temperature dependence of the corresponding integrated intensity is shown in Fig. 3b. It is smooth, without any phase transitions up to at least 320 K. Polarization analysis of the diffracted intensity shows both  $\sigma - \pi'$  and  $\sigma - \sigma'$  contributions. The azimuthal dependence of both components at  $L_{II}$  is shown in Fig. 4a, while Fig. 4b shows the energy dependence of the total scattered intensity at three characteristic temperatures. The latter is similar to the one of the (100) reflection at low temperatures, with two resonance peaks at  $L_{II}$  and  $L_{II}'$ , but the features observed above the edge are more pronounced here. Again, no off-resonance intensity is found at (110).

The different temperature, polarization, and azimuthal angle dependences of the intensities at (100) and (110) at  $L_{II}$  suggest that they have different origins. Previous work on 3d TMOs has demonstrated that cooperative tilts of the metal oxide octahedra can give rise to resonance effects at positions not allowed by the space

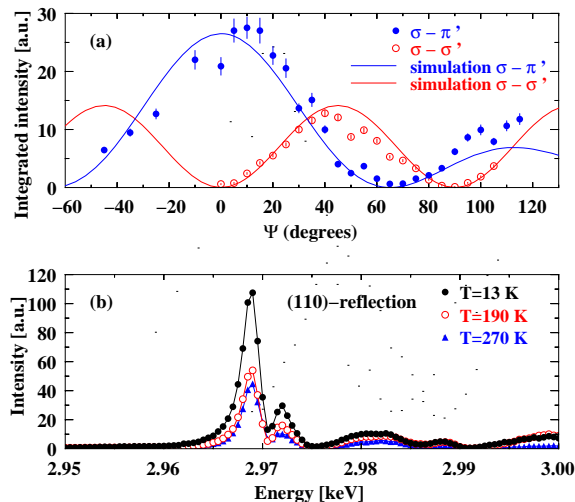


FIG. 4: (a) Azimuthal angle ( $\psi$ ) dependence of the scattered intensity of the (110) peak for both  $\sigma - \pi'$  (full bullets) and  $\sigma - \sigma'$  (empty bullets) polarization channels at  $T=13$  K. The solid lines are simulations of the scattered intensity induced by the tilting of the  $\text{RuO}_6$  octahedra. (b) Energy dependence of the (110) peak intensity at  $\psi = 0^\circ$  without analyzer for different temperatures. The data were corrected for absorption.

group [3], and powder neutron diffraction has shown that the  $\text{RuO}_6$  octahedra in  $\text{Ca}_2\text{RuO}_4$  are indeed tilted [17]. Based on the observed tilting pattern and following Ref. 3, the azimuthal dependence of both  $\sigma - \pi'$  and  $\sigma - \sigma'$  components at (110) was computed (solid curves in Fig. 4a). The result is in good agreement with the data. Further, the smooth temperature dependence of the tilt angles determined by neutron diffraction [17] is in accord with the lack of any anomalies observed in the (110) intensity up to at least 320 K. This indicates that the (110) peak is due to octahedral tilts. The same effect is also expected to give some contribution to the intensity in the  $\sigma - \pi'$  polarization channel at (100). This may be the origin of the weak intensity remaining above  $T_{\text{OO}}$  at this position (Fig. 3a).

Finally, we discuss the origin of the resonance peak observed at  $L_{\text{II}}'$ , 4 eV above the  $L_{\text{II}}$  edge. As indicated by the absorption-corrected energy scans at (100) displayed in Fig. 3c, the intensity at this energy is much more weakly temperature dependent than the one at  $L_{\text{II}}$ . A detailed series of measurements shows that the integrated intensity decreases gradually with increasing temperature and does not show any anomalies up to 320 K (Fig. 3b). This suggests that the higher-energy resonance peak arises from transitions into unoccupied orbitals not participating in the orbital ordering transition. Based on band structure calculations, according to which the crystal field splitting between the  $t_{2g}$  and  $e_g$  levels is about 4 eV [24], these can be identified as the Ru  $e_g$  orbitals.

In conclusion, a pronounced resonant enhancement of the scattered intensity is observed in  $\text{Ca}_2\text{RuO}_4$  at

the  $L_{\text{II}}$  and  $L_{\text{III}}$  absorption edges of ruthenium. Resonant diffraction measurements at the  $L_{\text{II}}$  edge reveal a sequence of phase transitions including the previously known magnetic transition at  $T_{\text{N}} = 110$  K, as well as a new transition at  $T_{\text{OO}} = 260$  K. The polarization and temperature dependence of the intensity, combined with supplementary  $\mu\text{SR}$  experiments, indicate that the latter transition originates from ordering of the 4d  $t_{2g}$  orbitals. At the orbital ordering wave-vector no charge scattering due to lattice distortions is observed. This illustrates the power of resonant x-ray diffraction to elucidate electronically driven orbital ordering phenomena that are only weakly coupled to the crystal lattice.

We acknowledge stimulating discussions with G. Khalullin and technical support from the staff at PSI. Use of the Advanced Photon Source is supported by the U.S. Department of Energy, Office of Basic Energy Sciences, under contract W-31-109-Eng-38. Work at Brookhaven was supported by the U.S. Department of Energy, Division of Materials Science, under Contract No. DE-AC02-98CH10886. Work at Kyoto was supported in part by Grants-in-Aid of Scientific Research from JSPS.

- 
- [1] Y. Maeno *et al.*, Nature **372**, 532 (1994).
  - [2] S. Nakatsuji and Y. Maeno, Phys. Rev. Lett. **84**, 2666 (2000); Phys. Rev. B **62**, 6548 (2000)
  - [3] H. Nakao *et al.*, Phys. Rev. B **66**, 184419 (2002).
  - [4] Y. Murakami *et al.*, Phys. Rev. Lett. **81**, 582 (1998).
  - [5] S. Grenier *et al.*, Phys. Rev. B **69**, 134419 (2004).
  - [6] A. Stunault *et al.*, Phys. Rev. B **60**, 10170 (1999).
  - [7] S. B. Wilkins *et al.*, Phys. Rev. Lett. **90**, 187201 (2003).
  - [8] S. Dhesi *et al.*, Phys. Rev. Lett. **92**, 056403 (2004).
  - [9] K. J. Thomas *et al.*, Phys. Rev. Lett. **92**, 237204 (2004).
  - [10] D. F. McMorrow, S. E. Nagler, K. A. McEwen, and S. D. Brown, J. Phys.: Condens. Matter **15**, L59 (2003).
  - [11] S. Nakatsuji, S. Ikeda, and Y. Maeno, J. Phys. Soc. Jpn. **66**, 1868 (1997).
  - [12] T. Mizokawa *et al.*, Phys. Rev. Lett. **87**, 077202 (2001).
  - [13] T. Hotta and E. Dagotto, Phys. Rev. Lett. **88**, 017201 (2002).
  - [14] V. I. Anisimov *et al.*, Eur. Phys. J. B **25**, 191 (2002).
  - [15] J. S. Lee *et al.*, Phys. Rev. Lett. **89**, 257402 (2002).
  - [16] J. H. Jung *et al.*, Phys. Rev. Lett. **91**, 056403 (2003).
  - [17] M. Braden, G. André, S. Nakatsuji, and Y. Maeno, Phys. Rev. B **58**, 847 (1998).
  - [18] C. S. Alexander *et al.*, Phys. Rev. B **60**, R8422 (1999).
  - [19] O. Friedt *et al.*, Phys. Rev. B **63**, 174432 (2001).
  - [20] G. Cao *et al.*, Phys. Rev. B **56**, R2916 (1997).
  - [21] H. Fukazawa and Y. Maeno, J. Phys. Soc. Japan **70**, 460 (2001).
  - [22] J. Hannon, G. Trammell, M. Blume, and D. Gibbs, Phys. Rev. Lett. **61**, 1245 (1988).
  - [23] J. Hill and D. McMorrow, Acta Cryst. A **52**, 236 (1995).
  - [24] Z. Fang, N. Nagaosa, and K. Terakura, Phys. Rev. B **69**, 045116 (2004).
  - [25] N. Bernhoeft *et al.*, Phys. Rev. Lett. **81**, 3419 (1998).
  - [26] N. Bernhoeft, Acta Cryst. A **55**, 274 (1999).

[27] T. Brückel *et al.*, Eur. Phys. J. B **19**, 475 (2001).